Available online at www.sciencedirect.com

SCIENCE DIRECT®

Polymer 45 (2004) 1439–1446

polymer

www.elsevier.com/locate/polymer

Elaboration of gradient structure materials from homogeneous system combining UV and thermal processes

N. Désilles, L. Lecamp, P. Lebaudy, C. Bunel*

UMR CNRS 6522 Polymères, Biopolymères, Membranes. Laboratoire de Matériaux Macromoléculaires, Institut National des Sciences Appliquées de Rouen,
Place E. Blondel, BP 08, 76131 Mont Saint Aignan Cédex, France

Received 7 October 2003; received in revised form 8 December 2003; accepted 8 January 2004

Abstract

A new synthesis of a gradient structure material from a homogeneous system of monomers is described. This synthesis involved 1,6-hexanediylbis[oxy(2-hydroxy-3,1-propanediyl)]bisacrylate, a hydroxytelechelic polybutadiene, and 4,4′-methylene-bis (cyclohexylisocyanate). In a first step, an acrylic double bonds photopolymerization gradient is created under UV exposure thanks to the decay of UV light intensity through the sample thickness. In a second step, a thermal crosslinking reaction is realised to form a polyurethane network in order to set the obtained gradient. The required experimental conditions to obtain and keep the gradient were investigated by FTIR and UV spectroscopies. Thus, a 50% 1,6-hexanediylbis[oxy(2-hydroxy-3,1-propanediyl)]bisacrylate double bonds conversion gradient was obtained in the ultimate 5 mm thick material. DMA and swelling analysis well revealed a difference of structures between both sides of the material, and a change in polarity was observed by contact angle measurements.

Keywords: Gradient structure material; Photopolymerization; Acrylate network

1. Introduction

Gradient polymers are mixtures of crosslinked polymers in which the concentration of one of the networks varies across the section of the material [1]. These multicomponent polymer systems then exhibit a composition or a structure that varies continuously with the position in the sample. Thus, they can be defined as a combination of an infinite number of layers, each one being a full system with its own composition and properties. The main advantage of such gradient polymers is their possibility, due to their spatial gradient, of making polymer systems with customised properties for different applications [2–11].

Several methods to obtain a gradient polymer can be encountered in literature [12–15]. The more usual way is the sequential curing [16–23] in which one network is firstly swelled by the components of a second network formed in a second time by photopolymerization [24–27]. The gradient is obtained by preventing the swelling from reaching its equilibrium value.

Recently, we developed a new method to create gradient materials without using a mixture containing at least one polymer, but involving a photopolymerization reaction from a homogeneous system, that is to say a system of monomers and oligomers [28]. The principle depends on two steps. In the first one, a polymerization gradient is photochemically created and obtained thanks to the variation of UV absorbance in the medium. The second step consists in setting the obtained gradient by a thermal crosslinking reaction. These first experiments showed the feasibility of gradient polymers using this new technique, but were not satisfactory enough regarding the obtained gradient and subsequently the resulting property gradient. With this aim in view, we chose to change the acrylate monomer, 2-hydroxyethyl methacrylate, for 1,6-hexanediylbis[oxy(2-hydroxy-3,1-propanediyl)] bisacrylate, well known to react radically under UV exposure thanks to its double bonds, and provided with chemical functions, namely hydroxyl groups, able to react thermally with another monomer in the second step. Concerning the thermal step, a polyurethane network will be formed using a multifunctional hydroxy oligomer (hydroxy telechelic polybutadiene), a di-isocyanate (4,4′-methylene-bis(cyclohexylisocyanate)), and the

---

[*] Corresponding author. Tel./fax: +33-2-35-52-84-46.
E-mail address: claude.bunel@insa-rouen.fr (C. Bunel).

0032-3861/$ - see front matter © 2004 Elsevier Ltd. All rights reserved.
doi:10.1016/j.polymer.2004.01.004

aforementioned 1,6-hexanediylbis[oxy(2-hydroxy-3,1-propanediyl)]bisacrylate. Thus, unlike common methods, that lead to interpenetrating polymer networks (IPNs), this new method will enable us to synthesize a material in which all monomers and oligomers will react in different ways along the thickness to result in only one network.

First of all, the required experimental conditions to obtain a gradient by UV irradiation will be determined. Afterwards, the polyurethane formation parameters enabling this gradient to be kept will be set. Then, the formation kinetics of the material will be investigated. And finally, the resulting properties of this gradient material will be analysed.

2. Experimental

2.1. Materials

Fig. 1 shows the chemical formula of the reactants used. Polybutadiene (Poly Bd R20LM®-HTPB) and 4,4′-methylene-bis(cyclohexylisocyanate) ($H_{12}MDI$) were kindly supplied, respectively, by Atofina and Bayer. HTPB is a low molar mass polybutadiene ($\overline{M_n} = 1370\ g\ mol^{-1}$) and presents an average hydroxy functionality $\overline{f_{OH}} = 2.45$. Microstructure studies indicate 22% of 1,2 units (vinyl units) and 78% of 1,4 units [29]. $H_{12}MDI$ and 1,6-hexanediylbis [oxy(2-hydroxy-3,1-propanediyl)]bisacrylate (HHPA) (Aldrich) were used as received. Dibutyl tin dilaurate (DBTL) (Aldrich), 2,2-dimethyl-2-hydroxyacetophenone (Darocur 1173) (Ciba Specialty Chemicals) and Tetrahydrofuran (THF) (Acros) were used without further purification.

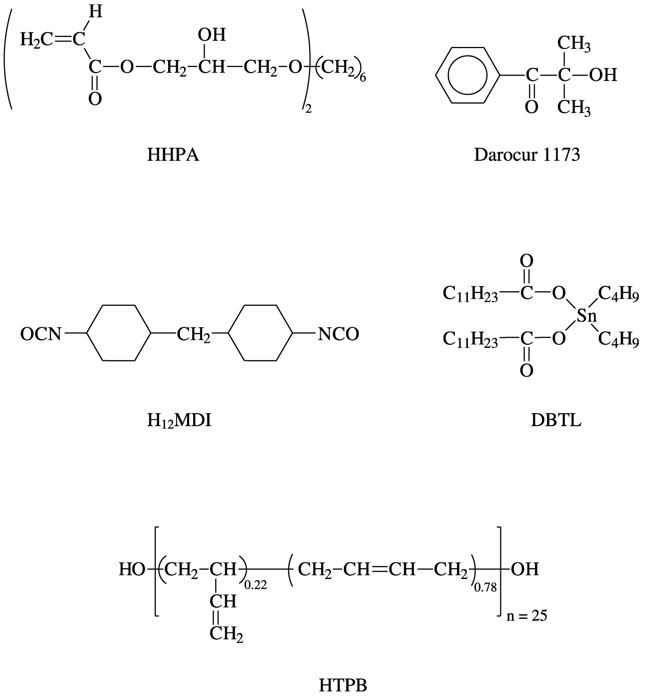
HHPA

Darocur 1173

$H_{12}MDI$

DBTL

HTPB

Fig. 1. Chemical formula of the reactants used.

2.2. Preparation of samples

HTPB and HHPA were first degassed for 1 h by a graduated vacuum up to 10^{-1}–10^{-2} mm Hg, respectively, at 80 and 30 °C in order to eliminate all volatile products. 28 mmol (38.4 g) of HTPB were introduced into a 250 ml round bottom flask equipped with a mechanical stirrer (300 rpm), a switchable inlet for nitrogen and a vacuum connector. Then the reactor was placed at room temperature under nitrogen. 34.2 mmol (12.8 g) of HHPA containing 0.15% (w/w) of Darocur 1173 (i.e. 10^{-2} mol l^{-1} compared to the acrylate monomer, and 0.028% (w/w) compared to the final mixture) and 68.3 mmol (17.9 g) of $H_{12}MDI$ were added and the mixture was stirred for 20 min. The high viscosity resulting mixture was degassed for 20 min by a graduated vacuum up to 10^{-1}–10^{-2} mm Hg at 30 °C to get rid of all the nitrogen bubbles created when stirring. This mixture was stored at − 18 °C until its use. Catalyst (DBTL) (2.4 mmol l^{-1}) was finally introduced carefully as rapidly as possible and just before the use of the reactional mixture returned to room temperature.

The mixture was then run in a mould of various thickness (up to 5 mm) as described in our previous work [28]. UV radiation is applied 4 min after introduction of the DBTL catalyst into the reactional mixture, in order to obtain proper homogenization under N_2 atmosphere.

2.3. Photopolymerization conditions

The UV radiation comes from a 350 W Oriel mercury vapour lamp. Its intensity is measured at the sample level by using a spectroradiometer (Intraspec II Oriel) of which probes are centred on 254, 312 or 365 nm. The radiation is monochromatic by means of the use of interferential filters (254, 289, 312, 334 or 365 nm).

2.4. Thermal crosslinking conditions

The sample unit is placed in a oven at a given temperature and crosslinking was allowed to proceed until complete disappearance of isocyanate functions.

2.5. Measurements

2.5.1. Real time infrared spectroscopy (RTIR)

Photochemical and thermal polymerization reactions were followed by RTIR (Perkin Elmer FTIR 2000 spectrometer) in attenuated total reflection (ATR). In case of films, a sample drop was deposited and spread out over the ATR diamond crystal with a quartz filter. This diamond crystal can be carried at a chosen temperature by a thermocouple. In case of thick materials, the samples were realized as shown in Scheme 1, the diamond crystal

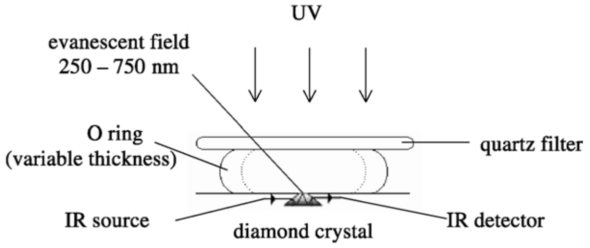

Scheme 1. Schematic shape of the analytical ATR device.

constituting the lower face of these samples. UV radiation from a 350 W Oriel mercury vapour lamp was introduced into the FTIR spectrometer sample chamber by a flexible light guide so that it did not interfere with the IR beam. The monochromatic UV radiation intensity was 6.5 mW/cm^2 at the sample level at 312 nm.

The disappearance of HHPA acrylic C=C stretching vibrations at 809 cm^{-1}, HTPB vinyl C=C stretching vibrations at 910 cm^{-1}, and H_{12}MDI isocyanate vibrations at 2257 cm^{-1} was observed. A reference band in the spectrum was used at 2924 cm^{-1} to calculate conversions. After correction of the baseline, conversions of HHPA acrylic double bonds, HTPB vinyl double bonds and isocyanate groups can be calculated by measuring the absorbance at each time of the reaction and determined as follows:

$$\chi_{\mathrm{C=CHHPA}(t)} = \frac{\dfrac{A_0^{809}}{A_0^{2924}} - \dfrac{A_t^{809}}{A_t^{2924}}}{\dfrac{A_0^{809}}{A_0^{2924}}} \times 100$$

$$\chi_{\mathrm{NCO}(t)} = \frac{\dfrac{A_0^{2257}}{A_0^{2924}} - \dfrac{A_t^{2257}}{A_t^{2924}}}{\dfrac{A_0^{2257}}{A_0^{2924}}} \times 100$$

$$\chi_{\mathrm{C=C\ HTPB}(t)} = \frac{\dfrac{A_0^{910}}{A_0^{2924}} - \dfrac{A_t^{910}}{A_t^{2924}}}{\dfrac{A_0^{910}}{A_0^{2924}}} \times 100$$

where $\chi_{(t)}$ is the conversion of these reactive functions at t time, A_0 is the initial absorbance (before UV irradiation) and A_t is the absorbance of the functional groups at t time.

2.5.2. Ultraviolet spectroscopy

The spectral absorbance of the reactive mixture was measured in mass, in a 1 mm thick quartz cell, by using an UV–Visible spectrophotometer (Perkin Elmer Lambda 16).

2.5.3. Dynamic mechanical analysis (DMA)

Samples were analyzed by dynamic mechanical analysis (DMA 7 Perkin Elmer) in compression mode with stainless steel parallel plate probe (1 mm diameter), at 1 Hz frequency and 10 °C/min heating rate. The static and dynamic forces applied were, respectively, 220 and 200 mN. The evolution of tan δ was followed versus temperature.

2.5.4. Swelling in THF

Swelling measurements were performed in THF at room temperature for 1, 24 and 72 h. After having weighed the swelled samples (m_s), they were dried at 60 °C until a constant mass was obtained (m_d). Swelling (Q) was then calculated using the following equation:

$$Q = \frac{m_s - m_d}{m_d} \times 100$$

2.5.5. Surface tensions

Surface tensions of both surfaces (upper and downer) of the material were evaluated by static contact angle (θ) measurements with three liquids: water, diiodomethane and ethylene glycol, using a GBX Digidrop ASE goniometer.

According to Owens–Wendt theory, the dispersive γ_s^d and polar γ_s^p components of the surfaces were determined:

$$\frac{(1+\cos\theta_i)\gamma_i}{2\sqrt{\gamma_i^d}} = \sqrt{\gamma_s^p} \times \sqrt{\frac{\gamma_i^p}{\gamma_i^d}} + \sqrt{\gamma_s^d}$$

where γ_i, γ_i^d, γ_i^p are the solvent superficial tension parameters [30].

Furthermore, the polarity of each side can be computed according to:

$$P = \frac{\gamma_s^p}{\gamma_s} \times 100$$

where γ_s is the material superficial tension ($\gamma_s = \gamma_s^p + \gamma_s^d$).

3. Results and discussion

3.1. Creation of the gradient under UV exposure

The decay of UV light intensity through the material thickness is the principle applied to create a polymerization gradient. Indeed, thanks to the sample absorbance and the distribution of light intensity through the irradiated system predicted by Beer–Lambert's law, an intensity gradient, and consequently a polymerization gradient, can be created inside the sample when exposed to UV radiation.

The investigation of suitable irradiation wavelength and material thickness has already been explained in detail in our previous work [28]. Taking into account the absorption spectrum in bulk of the reactive mixture (absorption due to Darocur 1173 and mainly to HHPA and HTPB), the irradiation wavelength was set to 312 nm, the intensity to 6.5 mW/cm^2 at 312 nm and the material thickness to 5 mm, in order to obtain a theoretical progressive decay of light intensity down to nearby 0 inside the sample.

A kinetic study monitored by FTIR was performed on a 5 mm thick sample with the above mentioned conditions in order to determine the appropriate irradiation time. At the surface, the conversion in double bonds was determined on a film applied on the ATR diamond crystal. In depth, the conversion was determined on the downer side of a 5 mm thick sample directly in contact with the ATR crystal. Fig. 2 shows that the HHPA double bonds conversion at the surface nearly reaches a maximum of 77% in about 15 min. But actually, the conversion in depth increases as soon as irradiation begins, and tends to a 20% conversion in depth in 15 min. This behavior is not in agreement with Beer–Lambert's law because the experimental conditions were chosen to obtain an intensity at the end of the 5 mm equal to zero (theoretical value of 3.10^{-7} mW/cm^2) so that the downer side should not be reached by UV radiation. Nevertheless, this phenomenon, that has already been encountered elsewhere [28,31,32], is not surprising and can be attributed to photobleaching. Thus, an irradiation that would not affect HHPA double bonds in depth would result in a very poor conversion in double bonds at the surface. That is the reason why we decided to set the irradiation time to 9 min, so that HHPA double bonds can react to a satisfactory level of about 70% at the surface, even if they react a little (around 15%) in depth.

3.2. Thermal crosslinking parameters of the polyurethane network

The second step consists in crosslinking the material, in order to avoid later evolution of the gradient. This crosslinking involves $H_{12}MDI$ which, thanks to its isocyanate functions and the hydroxyl groups of HHPA and HTPB, will react via a classical polyurethane formation reaction. A stoechiometric ratio in isocyanate functions and hydroxyl groups was chosen. The polyurethane synthesis kinetics are well-known to be heat sensitive in order to increase the kinetic, even more in bulk polymerization.

On the other hand, acrylate double bonds can readily react if heated. The effect of temperature on the polyurethane network formation and the HHPA double bonds reaction was studied on a unirradiated film sample in Fig. 3, at 30 and 80 °C. As expected, the higher the temperature is, the faster the polyurethane formation is and the higher the ultimate conversion in isocyanate functions is, respectively, 80 and 88% at 30 and 80 °C. The same behavior is observed with HHPA double bonds. Indeed, a 80 °C temperature leads to a fast polymerization that reaches 35% in only 1 h and keeps on increasing. This temperature is definitely not convenient. As far as the 30 °C kinetic is concerned, HHPA double bonds still react but in a definitely more attractive manner. Indeed, HHPA double bonds reach a maximal conversion of only 15% in 4 h, and increasing the reaction time does not make the double bonds polymerize further. Thus, the 30 °C temperature appears to be the choice temperature to avoid, as far as possible, an important polymerization of HHPA double bonds in depth where these functional groups are the more available. Moreover, as shown in Fig. 2, the photopolymerization step already leads to a 15% HHPA double bonds conversion in depth in 9 min, so that the thermal step will not affect the double bonds. Indeed, we can suppose that thanks to its two hydroxyl groups on each molecule, the chemical structure of HHPA enables to incorporate this monomer directly into the polyurethane network and so reduces its mobility and the thermal reactivity of its double bonds.

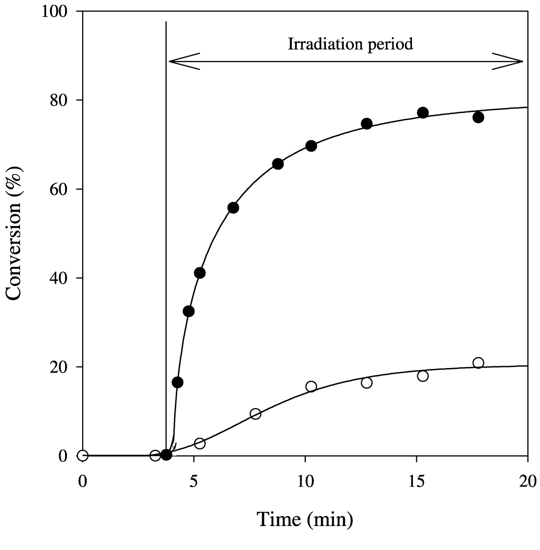

Fig. 2. Conversion of HHPA double bonds versus irradiation time at 30 °C at the surface (●) and at 5 mm (○).

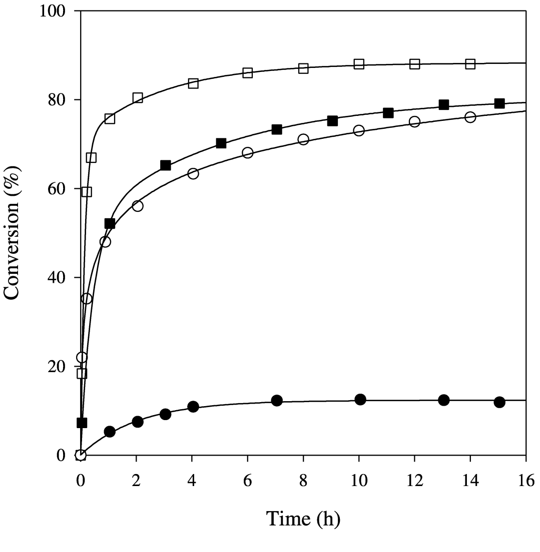

Fig. 3. Conversions of isocyanate functions, at 30 °C (■) and 80 °C (□), and HHPA double bonds at 30 °C (●) and 80 °C (○), for an unirradiated film sample versus time.

3.3. Study of the gradient material formation

The gradient polymer is now synthesized using the conditions previously mentioned. The conversions of isocyanate functions, HHPA double bonds, and HTPB vinyl double bonds at the surface and in depth are reported in Fig. 4.

Concerning HHPA double bonds, a 70% conversion at the surface and a 15% conversion in depth can be noticed, that is to say a 55% HHPA double bonds conversion gradient. Moreover, Fig. 4 shows that HTPB vinyl double bonds react in this first step, up to about 8% conversion at the surface and 6% in depth. Therefore, we can assume that HHPA undergoes a grafting reaction towards HTPB vinyl double bonds, what was already noticed in literature concerning other acrylate monomers [28,33,34]. Furthermore, we can suppose that the polymerization of HHPA can exhibit another crosslinking process through radical chain transfer mechanisms on hydroxyl groups, in addition to the obvious crosslinking by its two acrylate functions. Indeed, this phenomenon was mentioned concerning another acrylate monomer containing hydroxyl groups, 2-hydroxyethyl methacrylate [35–37]. Thus, as shown in Fig. 5, the UV step leads to a complex structure involving crosslinked HHPA homopolymer and crosslinking with HTPB, even more complex that H_{12}MDI starts reacting as soon as DBTL is introduced, that is to say 4 min before irradiation is switched on according to experimental conditions.

As far as isocyanate functions are concerned, their disappearance is a little bit slower at the surface than in depth. This can be explained by the polyHHPA network created more specifically in surface that makes the diffusion of reactive species more difficult. Thus, as introduced in Fig. 5, urethane functions can be created in depth between the isocyanate groups of H_{12}MDI and the hydroxyl groups of free HTPB and HHPA where they are more available, whereas at the surface they can be created between the isocyanate groups of H_{12}MDI and the hydroxyl groups of free and crosslinked HTPB and HHPA. Thanks to its two hydroxyl groups, HHPA is fully incorporated into the polyurethane network. Keeping in mind all these reactions, the resulting structure is very intricate and cannot be considered as an IPN. Furthermore, the reaction of isocyanate functions is far from being completed after 30 min, with only a 42% conversion at the surface and 46% in depth (Fig. 4).

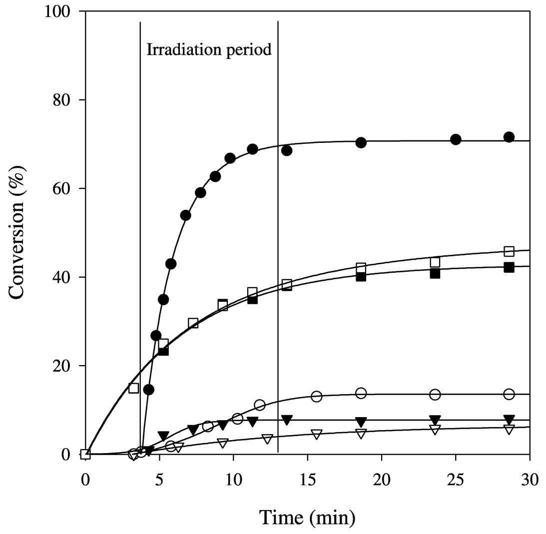

Fig. 4. Conversions of isocyanate functions at 30 °C at the surface (■) and in depth (□), HHPA double bonds at the surface (●) and in depth (○), and HTPB vinyl double bonds at the surface (▼) and in depth (▽), for a 5 mm thick sample versus time.

Time stability of the material was studied by determining the conversions of isocyanate functions, HHPA double bonds, and HTPB vinyl double bonds during 90 h at 30 °C (e.g. Fig. 6 for the bottom of the material). As expected, HHPA double bonds do not react in depth during the thermal crosslinking step. The same behavior is observed at the surface. We have therefore created and kept a 55% HHPA double bonds gradient that is stable as soon as irradiation is completed. Concerning isocyanate functions, a 75% conversion is obtained in depth after 4 days of reaction, whereas the surface exhibits a poor 60% conversion. Furthermore, the latter does not evolve further and is not sufficient enough to make sure of sample cohesion during removal from mould. Thus, another thermal step at higher temperature is required in order to reach an isocyanate conversion which will allow to remove the sample from the quartz filters.

For example, the conversions obtained during these thermal steps are reported for the depth of the material in Fig. 7. The sample is kept at 30 °C during 20 h, which corresponds to the time for which the isocyanate conversion nearly reaches a maximum. Then, the oven temperature is set to 60 °C during 24 h, thus leading to a 77% isocyanate conversion in depth and a 66% conversion at the surface. Thereby, the sample can be removed from the quartz filters very easily. Finally, the sample is placed and kept in a 30 °C oven during 5 days to allow complete reaction of unreacted isocyanate functions with atmospheric moisture. During this process, the HHPA double bonds conversion has increased up to 28% in depth and 78% at the surface.

Finally, a 5 mm thick gradient material was cut into 0.58 mm thick layers and the conversion in HHPA double bonds was measured by ATR for both sides of each layer. HHPA double bonds conversions plotted against thickness right after irradiation on material of variable thickness and in the ultimate material are presented in Fig. 8. We can notice that the gradient ultimately obtained is quite similar to the expected one. Indeed, the expected 55% HHPA conversion gradient has turn into a very satisfactory 50% gradient, with 78% conversion at the surface and 28% in depth. Furthermore, the ultimate material is stable through time after the whole process described above and further irradiation does not affect this gradient.

A DMA analysis was carried out on each layer

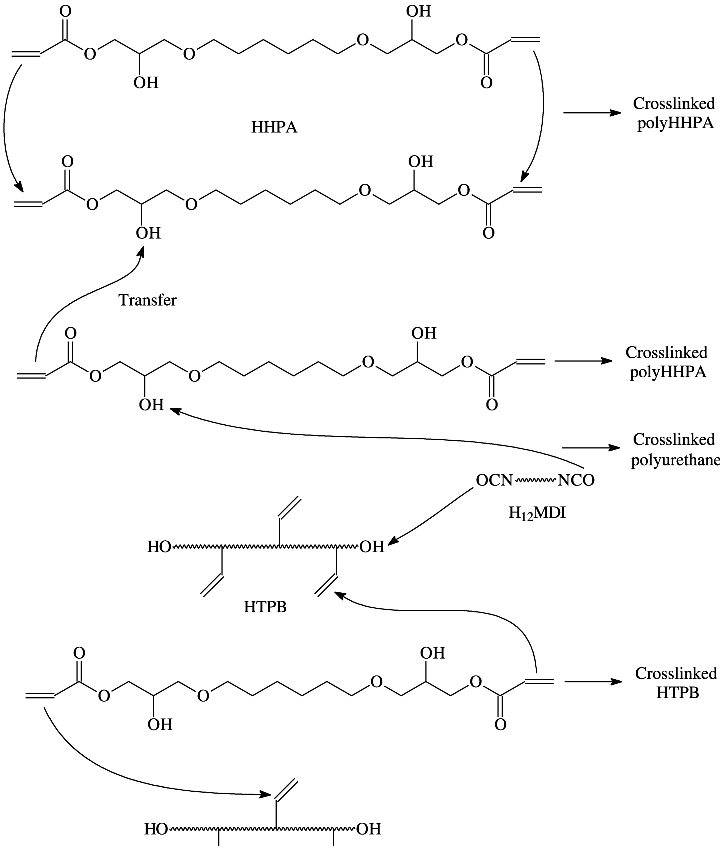

Fig. 5. Reaction scheme during photopolymerization step.

previously mentioned. The tan δ curves are shown in Fig. 9. An important point lies in the behavior of the layers around 60 °C. Indeed, this relaxation is not the homopolyHHPA one of which transition was observed at lower temperature (around 7 °C), but could be associated to the transition of polyHHPA acrylate backbone crosslinked by H_{12}MDI. This transition decreases through the thickness and tends to disappear in the bottom layers. This more important crosslinking density at the surface was checked by swelling the layers in THF, which revealed a higher swelling in depth

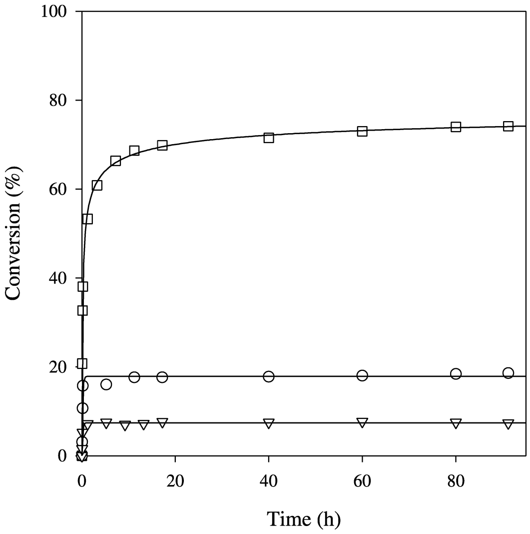

Fig. 6. Conversions in depth of isocyanate functions (□), HHPA double bonds (○), and HTPB vinyl double bonds (▽), for a 5 mm thick irradiated sample versus time at 30 °C.

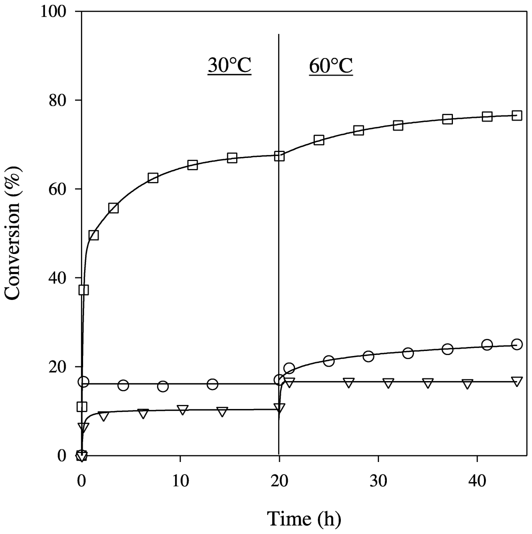

Fig. 7. Conversions in depth of isocyanate functions (□), HHPA double bonds (○), and HTPB vinyl double bonds (▽), for a 5 mm thick irradiated sample versus time: 20 h at 30 °C followed by 24 h at 60 °C.

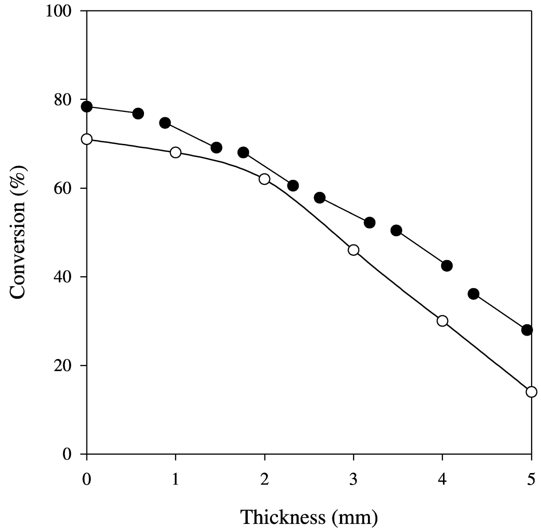

Fig. 8. Comparison of HHPA double bonds conversion right after irradiation at 30 °C on material of various thickness (○) and in both sides of the ultimate material layers (●–●).

(175%) than at the surface (140%). As far as the other relaxations observed are concerned, the one seen around − 40 °C does not vary significantly when thickness increases and can be assigned to HTPB soft segments. Furthermore, the mechanical analysis exhibits an intermediary transition around 17 °C which increases with thickness. This transition can be attributed to the polyurethane network made of HTPB, H_{12}MDI, and HHPA, this diol acting like a chain extender. On top of that, the bottom layers present a more narrow transition, in opposition with the broad transition of the surface. This phenomenon indicates a more homogeneous structure in depth than at the surface, as expected when considering the reaction scheme. To sum up, the structures of the created networks seem to be different at the surface and in depth.

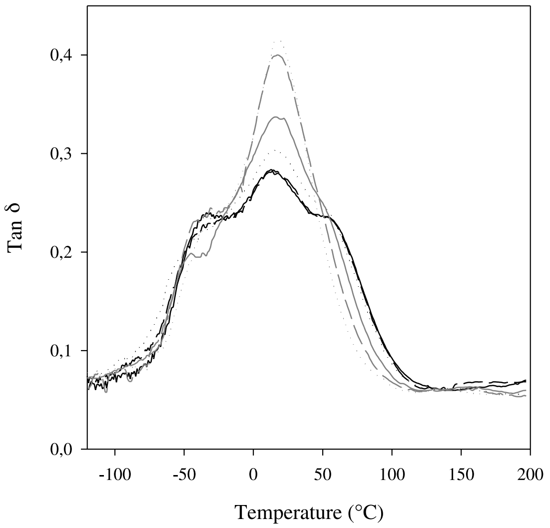

Fig. 9. Tan δ curves versus temperature for different layers, with incident beam on layer 1 (solid black layer 1, dashed black layer 2, dotted black layer 3, solid grey layer 4, dashed grey layer 5, dotted grey layer 6).

Polarity of both sides of the sample was calculated by means of contact angle measurements. Thus, the surface exhibits a polarity $P_{\mathrm{surf}} = 28\%$ ($\theta_{\mathrm{water\ surf}} = 68°$), whereas the depth one is only $P_{\mathrm{depth}} = 18\%$ ($\theta_{\mathrm{water\ depth}} = 76°$). As far as homopolyHHPA is concerned, a 30% polarity was computed according to the same method ($\theta_{\mathrm{water\ pHHPA}} = 64°$). Therefore, the surface is very close to homopolyHHPA in terms of polarity.

4. Conclusion

In this study, a material presenting a polymerization gradient was successfully obtained from a homogeneous system composed of HHPA, HTPB, and H_{12}MDI using photopolymerization. The thermal crosslinking of the medium, required to set the gradient, did not affect the aforementioned gradient, but a supplementary thermal step was carried out to enable an easy removal of the material from the quartz filters, which resulted in a small decrease of the double bonds gradient from 55% initially down to 50% finally. The use of a difunctional hydroxy acrylate ended up with no stability problem during the thermal step like encoutered before [28]. Moreover, the ultimate gradient material obtained is stable against later UV exposure, and presents a structure gradient through the thickness due to different network structures and crosslinking densities. On top of that, a polarity gradient was obtained, with a surface near to polyHHPA in terms of polarity.

References

[1] Sperling L. Interpenetrating polymer networks and related materials. New York: Wiley; 1981.
[2] Milczarek P, Kryszewski M. Prog Colloid Polym Sci 1985;71:96.
[3] Milczarek P, Kryszewski M. Colloid Polym Sci 1987;265:481.
[4] Pluta M, Milczarek P, Kryszewski M. Colloid Polym Sci 1987;265: 490.
[5] Xie XM, Matsuoka M, Takemura K. Polymer 1992;33:1996.
[6] Akovali G, Biliyar K, Shen M. J Appl Polym Sci 1976;20:2419.
[7] Jasso CF, Hong SD, Shen M. Am Chem Soc Adv Chem Ser Multiphase Polym 1979;23:444.
[8] Martin GC, Enssani E, Shen M. J Appl Polym Sci 1981;26:1465.
[9] Shen M, Bever MB. J Mater Sci 1972;7:741.
[10] Dror M, Elsabee MZ, Berry GC. J Appl Polym Sci 1981;26:1741.
[11] Mueller KF, Heiber SJ. J Appl Polym Sci 1982;27:4043.
[12] Koike Y, Tanio N, Nihei E, Ohtsuka Y. Polym Engng Sci 1989;29: 1200.
[13] Wang DJ, Gu CB, Chen PL, Liu SX, Zhen Z, Zhang JC, Liu XH. J Appl Polym Sci 2003;87(2):280.
[14] Agari Y, Shimada M, Ueda A, Nagai S. Macromol Chem Phys 1996; 197:2017.
[15] Murayama S, Kuroda S, Osawa W. Polymer 1993;34(18):3893.
[16] Karabanova LV, Sergeeva LM, Lutsyk ED, Kuznetsova VP. Polym Sci, Ser A 1996;38(10):1108.
[17] Jasso CF, Martinez JJ, Mendizabal E, Laguna O. J Appl Polym Sci 1995;58:2207.
[18] Karabanova L, Pissis P, Kanapitsas A, Lutsyk E. J Appl Polym Sci 1998;68:161.

[19] Akovali G. J Appl Polym Sci 1999;73:1721.

[20] Sorm M. La Technique Moderne 1988;80(7–8):19.

[21] Ohtsuka Y. Appl Phys Lett 1973;23(5):247.

[22] Dror M, Elsabee MZ, Berry GC. Biomat Med Dev Art Org 1979;7(1):31.

[23] Beauregard GP, James SP. Biomed Sci Instrum 1999;35:415.

[24] Lipatov YS, Karabanova LV, Gorbach LA, Lutsyk ED, Sergeeva LM. Polym Int 1992;28:99.

[25] Elsabee MZ, Dror M, Berry GC. J Appl Polym Sci 1983;28:2151.

[26] Jasso CF, Valdéz J, Pérez JH, Laguna O. J Appl Polym Sci 2001;80:1343.

[27] Lipatov YS, Karabanova LV. J Mater Sci 1995;30:1095.

[28] Désilles N, Lecamp L, Lebaudy P, Bunel C. Polymer 2003;44(20):6159.

[29] Poletto S, Pham QT. Macromol Chem Phys 1994;195:3901.

[30] Windrop++Software, from GBX Digidrop ASE Goniometer.

[31] Rutsch W, Dietliker K, Leppard D, Kölher M, Misev L, Kolczak U, Rist G. Prog Org Coatings 1996;27:227.

[32] Miller GA, Gou L, Narayanan V, Scranton AB. J Polym Sci, Part A 2002;40(6):793.

[33] Huang NJ, Sundberg DC. J Polym Sci, Part A 1995;33:2587.

[34] Mateo JL, Calvo M, Bosch P. J Polym Sci, Part A 2001;39:2444.

[35] Gregonis DE, Russell GS, Andrade JD, de Visser AC. Polymer 1978;19:1279.

[36] Montheard JP, Chatzopoulos M, Chappard D. J Macromol Sci—Rev Macromol Chem Phys 1992;C32(1):1.

[37] Morra M, Occhiello E, Garbassi FJ. J Colloid Interface Sci 1992;149:84.